DOI: 10.61782/fa.2023.0746

forum acusticum 2023

NUMERICAL MODELLING OF A PHASE-GRADIENT LINING USING A METAFLUID MODEL

Giorgio Palma* **Lorenzo Burghignoli** **Umberto Iemma**
Department of Civil, Computer Science and Aeronautical Technologies Engineering,
University of Roma Tre, Italy

ABSTRACT

This contribution presents the modelling of a phase-gradient metamaterial for the surface treatment of the internal walls of a turbofan nacelle intake. The metamaterial is modelled through a metafluid, whose bulk modulus and inertia tensor are determined by a simulation-based numerical optimization, minimizing the acoustic emission from the duct inlet. The flow and its interaction with both the nacelle and lining are modelled in a simplified way using a potential flow over smooth surfaces. The parameters of the metafluid are tailored to tackle the incident field expressed in terms of duct modes propagating from the fan section for the blade passage frequency. Numerical results show the encouraging capabilities of a phase-gradient device to change the directivity of the noise radiated by an aeronautic turbofan nacelle, abating the propagation of a duct mode linked to a relevant noise generation mechanism.

Keywords: *Metafluid, Metamaterial, Metasurfaces, Aeroacoustics, Liners).*

1. INTRODUCTION

An increasing interest is arising around the potential of metamaterials in aeroacoustics during the last decade, as indicated [1, 2] and shown in several dedicated works aimed at the extension of existing acoustic models to handle the presence of flow convection [3–7]. Recent studies on a particular class of metamaterials, identified as phase-gradient metasurfaces (PGMSs) and devoted to sound redistribution rather than absorption, numerically demonstrated the possibility to significantly change the noise emission directivity of simple 2D rectangular ducts [8, 9].

This paper intends to numerically analyse the potential benefits of the PGMS metamaterial treatment class in a simplified, realistic setting that includes the essential features seen in industrial applications. Specifically, the PGMS metafluid model is here applied for the numerical analysis of the effect of a PGMS-lining of the inlet of a reference turbofan, which geometry is comparable with the modern high-bypass ratio engines, aimed at the reduction of fan noise in conditions comparable to take-off operations of civil, commercial aircraft in terms of unperturbed Mach number. Numerical predictions are obtained through Finite Element Method (FEM) simulations solving for the velocity potential in an irrotational flow, describing the acoustic source in terms of hard-walled annular duct modes at the fan section. In addition, a numerical analysis determines the modal content at the fan section for the frequency of interest (the BPF) that propagates through the nacelle inlet interacting with the metamaterial lining.

A simulation-based optimization determines the metafluid design, minimizing the acoustic pressure level over an arc of receivers surrounding the nacelle inlet. To describe a incident field representative of take-off operations, the modal components are defined on a statistical basis with uniform random distributions of amplitudes and phases, with the rotor-locked mode power level set to be dominating over the multimodal content.

Eversman [10] showed that equivalent impedances of linings attenuating tones at the BPF are characterized by high resistance values, on the contrary, numerical simu-

***Corresponding author**: giorgio.palma@uniroma3.it.*

lations show that a PGMS lining has the potential to attenuate the considered mode with a different mechanism, since no dissipation is included in the model nor in the metafluid.

2. THE PGMS EQUIVALENT METAFLUID

The physical mechanism on which PGMSs are based is the introduction of a controlled phase delay $\Delta\phi = \phi_{ms} - \phi_{hw}$ in the acoustic field transmitted or reflected from the lined boundary compared to an acoustically transparent or rigid boundary, respectively. For a reflective metasurface, this term is part of the generalized reflection law, also called generalized Snell's law for reflection (or simply GSL)

$$\sin\theta_r = \frac{\lambda}{2\pi}\frac{\partial}{\partial\zeta}\Delta\phi(\zeta,\lambda) + \sin\theta_i \tag{1}$$

with λ the wavelength of the incident acoustic perturbation, θ_i and θ_r the angles of the incident and reflected fields. For periodic distributions of phase delays, an additional term depending on the spatial period Γ should be included, and in case of partitioning of the metasurface in cells of width w a further one has to be considered, to account for higher diffraction orders [11]:

$$\sin\theta_r = \frac{\lambda}{2\pi}\frac{\partial}{\partial\zeta}\Delta\phi(\zeta,\lambda) - m\frac{\lambda}{\Gamma} - n\frac{\lambda}{w} + \sin\theta_i \quad m,n\in\mathcal{Z} \tag{2}$$

In the directions where the delay presents a gradient, the reflection angle of the acoustic field can be effectively modified by the metasurface. The acoustic *metabehaviour* typically pursued with a PGMS is hence a redistribution of the acoustic energy, such as sound focusing, wave shape conversion (*e.g.* spherical to planar and viceversa) or extreme steering of acoustic reflection (up to the conversion of a perturbation into a surface wave). Several different designs have been developed for the elementary cells, with complex shapes to achieve subwavelength thicknesses or to maximise transmission/reflection efficiencies [12–16]. Focusing our attention on PGMS for reflection, all concepts are based on creating paths of tailored lengths for the incident wave, the simplest design for the single cell is hence a straight channel such that the delay is defined by

$$\Delta\phi(\zeta,\lambda) = -\frac{4\pi h(\zeta)}{\lambda} \tag{3}$$

An acoustic metafluid is a metamaterial that behaves acoustically as a fluid due to the null shear modulus exhibited by its structure. The propagation of an acoustic disturbance within the most general metafluid is effectively described by [17, 18]

$$-\frac{\partial^2 p}{\partial t^2} + c_{\text{ref}}^2\,\hat{\mathcal{K}}\,\nabla\cdot\left(\mathbf{Q}\,\hat{\boldsymbol{\varrho}}^{-1}\,\mathbf{Q}\,\nabla p\right) = 0 \tag{4}$$

where ϱ_{ref}, $\mathcal{K}_{\text{ref}}$, and $c_{\text{ref}} = \sqrt{\mathcal{K}_{\text{ref}}/\varrho_{\text{ref}}}$ are the reference density, bulk modulus, and speed of sound, respectively. $\mathbf{Q}$ can be any symmetric tensor such that $\nabla\cdot\mathbf{Q} = 0$, and $\boldsymbol{\varrho} = \hat{\boldsymbol{\varrho}}\varrho_{\text{ref}}$ represents the anisotropic inertia of the material, $\mathcal{K} = \hat{\mathcal{K}}\mathcal{K}_{\text{ref}}$, and the Cauchy stress tensor for such a material is given by $\boldsymbol{\sigma} = -p\,\mathbf{Q}$.

Following the Transformation Acoustics (TA) procedure [17], an expression for the inertia tensor, bulk modulus and $\mathbf{Q}$ such that a metafluid domain can mimic another region can be obtained. The first step is to set a coordinate transformation between the original domain Ω and the metafluid ω, by means of a invertible mapping $\Omega\to\omega$ defined by $\boldsymbol{\xi} = \chi(\boldsymbol{\Xi})$.

For the sake of simplicity, in the following the problem is addressed under the hypothesis of inertial metafluid, a special case of the more general class of metacontinua which implies that $\mathbf{Q} = \mathbf{I}$. In this case, the metafluid parameters are related to $\mathbf{F}$ by

$$\hat{\mathcal{K}} = \det\mathbf{F}, \quad \hat{\boldsymbol{\varrho}} = \det(\mathbf{F})(\mathbf{V}\mathbf{V}^{\mathrm{T}})^{-1} \tag{5}$$

with $\mathbf{F} = \mathbf{V}\mathbf{R}$ as defined by the polar decomposition, and its components are $f_{ij} = \partial\xi_i/\partial\Xi_j$ [17].

The present work analyzes the case of an axial symmetric geometry, in which one of the boundaries defining the revolution section includes a PGMS lining. In this configuration, the device can be considered a semi-local lining, as the channels are separated by septa in the axial direction but continuous along the circumference. A coordinate transformation is set for each i-th ring/cell.

Considering two sets of cylindrical coordinates, $\boldsymbol{\xi} = (r,\alpha,z)$ and $\boldsymbol{\Xi} = (R,A,Z)$ in the undeformed and deformed domain, respectively, the transformation reads:

$$\begin{aligned} R - r_0(z) &= \frac{h_{ms}}{h_i}\left(r - r_0(z)\right) \\ A &= \alpha \\ Z &= z \end{aligned} \tag{6}$$

indicating with $r_0(z)$ the inner radius of the lined wall, which is, in general, a function of z, with h_i the height of the i-th undeformed ring and with h_{ms} the height of the metafluid lining, *i.e.* of the deformed channels.

The delay of Eq.(3) can then be expressed as a function of the bulk modulus of the equivalent metafluid for a given coordinate transformation:

$$\Delta\phi_i(\lambda) = \frac{4\pi g_1(\mathcal{K}_i)}{\lambda} \qquad (7)$$
$$\mathcal{K}_i = g_2\left(R, h_{ms}, h_i, r_0(z)\right)$$

It's worth noting that modelling the metasurface as an equivalent metafluid is efficient from a computational point of view, allowing to optimize the design with no need for updating geometry and mesh at each iteration.

3. NUMERICAL METHODS

The effect of the PGMS-equivalent metafluid is evaluated with numerical simulations of the aeroacoustic propagation from a nacelle inlet, focusing on the reduction of the noise radiated towards the ground during take-off operations.

The geometry of the inlet portion of the reference nacelle is built using the Class Shape Transformation (CST) method [19]. Figure 1 shows the main parameters defining the inlet geometry, which values, selected to obtain a nacelle representative of modern turbofans, are resumed in Tab.1: the length of the inlet L_n, the maximum radius of the cowling r_{max}, the fan section radius r_f, the height h_s and length L_s of the spinner cone; the PGMS lining is defined by the width w_{ms} and height h_{ms} of its rings, fixed in the number of eight in this study, and by its positioning along the inlet wall z_{ms}. The other relevant design parameters of the reference turbofan are defined in line with modern propulsion units. The number of blades of the fan disk is set $n_{fb} = 16$, and its maximum rotational speed $\omega_f = 2355$ rpm, hence the related BPF$_{max}$ of the reference fan is $f_{BPF} = 628Hz$.

An arc of virtual receivers surrounding the cowling, centered on the fan section with radius $r_{mic} = 3.5m$ $(2.06r_f)$ and extending from 20° to 120° (being 0° aligned with z-direction of Figure 1), is defined for the evaluation of the lining effect on the radiated field. The fluid around the nacelle is modelled as a barotropic inviscid and irrotational medium, with an unperturbed Mach number $Ma = 0.2$ compatible with the take-off speed of commercial aircraft. The background flow around the surfaces $\mathbf{v}_0$ (local velocity vector) is evaluated with a steady compressible potential solution, compatibly with

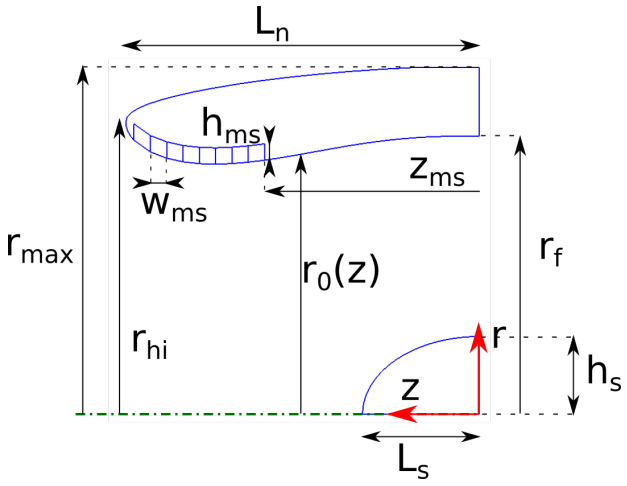

Figure 1: Sketch of the nacelle inlet geometry with the metalining.

Table 1: Values of geometric parameters defining the reference nacelle.

r_f	1.7 m	L_n	1.272 r_f
r_{max}	1.252 r_f	w_{ms}	0.7/8 λ_{BPF}
h_s	0.28 r_f	h_{ms}	0.1 m
L_s	1.5 h_s	z_{ms}	0.79 L_n

the above assumption. The propagation of acoustic perturbation under the mentioned hypotheses is ruled by the following equation for the acoustic velocity potential φ

$$-\frac{\partial}{\partial t}\left[\frac{\varrho_{\text{ref}}}{c^2_{\text{ref}}}\left(\frac{\partial\varphi}{\partial t} + \mathbf{v}_0\cdot\nabla\varphi\right)\right] + \nabla\cdot\left[\varrho_{\text{ref}}\nabla\varphi - \frac{\varrho_{\text{ref}}}{c^2_{\text{ref}}}\mathbf{v}_0\left(\frac{\partial\varphi}{\partial t} + \mathbf{v}_0\cdot\nabla\varphi\right)\right] = 0. \qquad (8)$$

The acoustic pressure is related to φ by the Bernoulli theorem

$$-p = \varrho_{\text{ref}}\left(\frac{\partial\varphi}{\partial t} + \mathbf{v}_0\cdot\nabla\varphi\right) \qquad (9)$$

In the metafluid domain, occupied by the lining rings, the solution for the acoustic pressure is held by Eq. (4), where the inertia tensor and bulk modulus for each ring are defined by Eq. (7). The rings are separated one to the other by acoustically rigid septa imposing the normal derivative of the acoustic velocity to be null on these internal boundaries, creating a *semi-local* lining which is non-local in the

circular direction. The rigid wall condition is also considered for all the non-lined boundaries of the nacelle and for the bottom of the metafluid rings. The boundary separating the outer and metafluid domains is considered to be aerodynamically impenetrable yet acoustically transparent. This simplifying assumption introduces a discontinuity in the background flow field, and is intended to model a covering with the described properties to avoid detrimental aerodynamic interference with the metafluid structure.

For the definition of the acoustic incident field, the hard-walled annular duct modes $U_{m,\mu}(r) = N_{m,\mu}S(\alpha_{m,\mu}r)$ at the fan section are evaluated numerically. At the fan section the flow can be considered with little approximation as uniform, such that the modal radial and axial wave numbers satisfy $\alpha^2_{m,\mu} = (\omega - Ma\, k_{m,\mu})^2 - k^2_{m,\mu}$, with $\beta = \sqrt{1-Ma^2}$. The modal shapes are imposed at the fan section (that extends from h_s to r_f) as sound sources and propagated in the duct, with amplitudes $N_{m,\mu}$ normalized such that [20]:

$$\int_{h_s}^{r_f} U^2_{m,\mu}(r) r\, dr = 1 \tag{10}$$

Separate calculations of the acoustic radiation are needed for each mode when evaluating the lining effect.

The aeroacoustic propagation problem stated above is evaluated with a commercial FEM solver in the frequency domain. The integrated weak formulations of Eqs.(4) and (8) are implemented in their Fourier-transformed version, along with the related boundary conditions completed with non reflecting conditions at the domain truncation implemented as Perfectly Matched Layers (PML) with polynomial coordinate stretching.

The acoustic pressures at the receivers' arc from the FEM simulations are used in an optimization process to identify the metafluid parameters that minimize the noise radiation. The incident field for the optimization considers the azimuthal mode m=16 at the BPF, associated in the analyzed case with only one radial mode with axial wave number $k_z = 2.6826$. The selected acoustic mode is the rotor-locked mode for the BPF, that is of primary importance during the take-off maneuver up to the cut-back, when the fan is rotating at its maximum speed and shock structures appear near the supersonic tip speed fan, dominating the forward-radiated fan acoustic spectrum [21–23]. In this work, the optimal metafluid is the one that minimizes the merit function defined as the integral of the Sound Pressure Level over the receivers' arc:

$$J(\mathbf{x},\mathbf{y}) = \int_{\mathcal{L}_{mic}} 10\log_{10}\left(\frac{p(\mathbf{x},\mathbf{y})^2}{p^2_{ref}}\right) dl \tag{11}$$

A Particle Swarm Optimization (PSO) algorithm [24] is used to search for the global minimum of the objective function. The optimization variables are the equivalent depths of the rings h^i_{ms}, which values are bounded to have $\Delta\phi^i(\lambda_{BPF})$ varying in a range of 2π. The optimal solution is then analyzed using each of the cut-on modes as incident field, and the results from simulations for each mode are then combined, considering random amplitudes and phases, in order to evaluate the overall lining effect at the BPF:

$$\begin{aligned} p_t(\mathbf{x},\omega) = &\sum_m \sum_{\mu(m)} \delta_{m\hat{m}} \hat{A}_{m,\mu}\hat{p}_{m,\mu}(\mathbf{x},\omega)e^{i\hat{\Phi}_{m,\mu}} \\ &+ \delta_{m\check{m}}\check{A}_{m,\mu}\check{p}_{m,\mu}(\mathbf{x},\omega)e^{i\check{\Phi}_{m,\mu}} \end{aligned} \tag{12}$$

where δ_{ij} is the Kronecker delta, the superscripts $\check{}$ and $\hat{}$ identify the rotor-locked mode and all the remaining modes, respectively.

4. RESULTS

The results of the optimization of the metafluid are shown in Table 2 in terms of $\Delta\phi$ and equivalent depths of the rings. It can be seen that the resulting acoustic treatment is characterized by a series of cells with non-uniform equivalent depths corresponding to the extreme values (box constraints) of $\Delta\phi$. Figure 2 shows a comparison between the

Table 2: Optimized ring depths

cell	h_i/λ_{BPF}	$\Delta\phi_i$
1	1	4π
2	0.5019	2.0076π
3	0.5017	2.0069π
4	1	4π
5	1	4π
6	0.9433	3.7732π
7	0.5165	2.0659π
8	0.9256	3.7024π

pressure fields obtained in the with and without acoustic treatment in both the cases where all the acoustic modes

are present (Figure 2a and Figure 2c) or only the rotor-locked mode (Figure 2b and Figure 2d). It can be seen

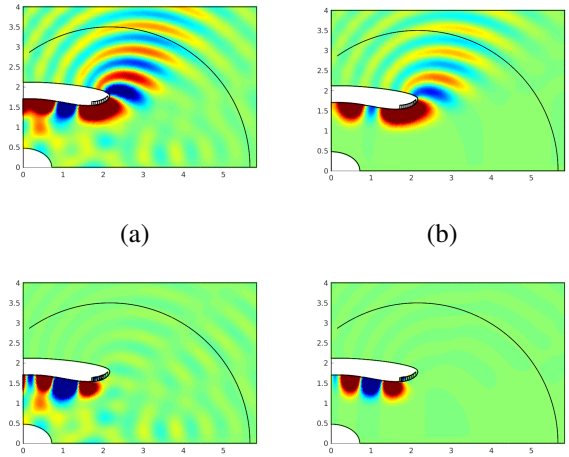

(a) (b) (c) (d)

Figure 2: Pressure fields for M=0.2: 2a and 2c all modes considered for non lined and lined inlet respectively, 2b and 2d rotor locked mode at BPF only for non lined and lined inlet respectively.

how the metasurface manages to drastically reduce the contribution of the rotor-locked mode and, albeit not significantly, also the rest of the acoustic modes. This result is not surprising, as only the rotor-locked mode has been included in the definition of the incident field in the optimization process. Quantitatively, the effect of acoustic treatment can be observed in Figure 3, in terms of Insertion Loss (IL) at the receivers arc for the BPF, the IL being defined as

$$IL\left(\theta, f_{BPF}\right) = 10\log_{10}\left(\frac{\left(\sum_{m,n} A^{ms}_{m,n} p^{ms}_{m,n}\right)^2}{\left(\sum_{m,n} A^{hw}_{m,n} p^{hw}_{m,n}\right)^2}\right). \tag{13}$$

The lines and the colored areas in Figure 3 represent the mean value and the 98% confidence interval respectively for the case of 1000 realizations. The presence of the proposed acoustic treatment causes a reduction of the acoustic field which for directivity angles greater than $50°$ (note that $\theta = 0°$ corresponds to the microphone in front of the fan) is of the order of 20dB. By comparing the dotted lines, corresponding to the analyzes carried out with and

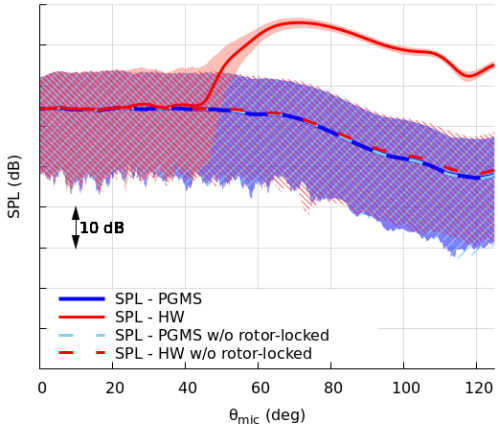

Figure 3: Results at the receivers arc for the BPF: Sound Pressure Level of non lined nacelle, in red, and in presence of the PGMS, in blue. Dashed lines are evaluated excluding the rotor locked mode from the analysis. For each line, the colored areas represent the 98% confidence interval.

without treatment in the absence of the rotor-locked mode, it can be observed once again how the metasurface is only marginally able to reduce the impact of the other acoustic modes.

5. SUMMARY

In this work a concept for an acoustic treatment for engine nacelles based on phase gradient metasurfaces modeled through equivalent metafluids is proposed. The obtained model is applied for the numerical analysis of the effect of an acoustic lining for the air intake of a reference high bypass ratio turbofan, considering an incident field obtained through an analysis of the acoustic modes present at the blade passage frequency. The parameters of the equivalent metafluids are determined through an optimization process aimed at reducing the acoustic field, obtained starting from an incident field consisting of the rotor-locked mode only, in an arch of microphones external to the air intake. The results obtained, although preliminary, show that phase gradient metasurfaces are potential candidates for the development of small-sized devices aimed at reducing fan noise.

6. REFERENCES

[1] G. Palma, H. Mao, L. Burghignoli, P. Göransson, and U. Iemma, "Acoustic Metamaterials in Aeronautics," *Applied Sciences*, vol. 8, p. 971, jun 2018.

[2] U. Iemma and G. Palma, "Spacetime-bending transformations in aeroacoustics," in *Proceedings of the 26th International Congress on Sound and Vibration, ICSV 2019*, Canadian Acoustical Association, 2019.

[3] U. Iemma and G. Palma, "Aeroacoustic design of metafluid devices," in *24th International Congress on Sound and Vibration 2017, ICSV 2017: London Calling*, 2017.

[4] U. Iemma and G. Palma, "On the use of the analogue transformation acoustics in aeroacoustics," *Mathematical Problems in Engineering*, vol. vol. 2017, p. 16 pages, 2017. Article ID 8981731.

[5] H. Ryoo and W. Jeon, "Effect of compressibility and non-uniformity in flow on the scattering pattern of acoustic cloak," *Scientific Reports*, vol. 7, no. 1, p. 2125, 2017.

[6] Y. He, S. Zhong, and X. Huang, "Extensions to the acoustic scattering analysis for cloaks in non-uniform mean flows," *The Journal of the Acoustical Society of America*, vol. 146, no. 1, pp. 41–49, 2019.

[7] U. Iemma and G. Palma, "Convective correction of metafluid devices based on taylor transformation," *Journal of Sound and Vibration*, vol. 443, pp. 238 – 252, 2019.

[8] G. Palma and L. Burghignoli, "On the integration of acoustic phase-gradient metasurfaces in aeronautics," *International Journal of Aeroacoustics*, vol. 19, no. 6-8, pp. 294–309, 2020.

[9] U. Iemma and G. Palma, "Optimization of metasurfaces for the design of noise trapping metadevices," in *Proceedings of the 26th International Congress on Sound and Vibration, ICSV 2019*, Canadian Acoustical Association, 2019.

[10] W. Eversman, "Effect of local impedance variation and non-linearity on multiple tone attenuation," *International Journal of Aeroacoustics*, vol. 14, no. 1-2, pp. 281–303, 2015.

[11] W. Wang, Y. Xie, B.-I. Popa, and S. A. Cummer, "Subwavelength diffractive acoustics and wavefront manipulation with a reflective acoustic metasurface," *Journal of Applied Physics*, vol. 120, no. 19, p. 195103, 2016.

[12] Y. Li, X. Jiang, R.-q. Li, B. Liang, X.-y. Zou, L.-l. Yin, and J.-c. Cheng, "Experimental realization of full control of reflected waves with subwavelength acoustic metasurfaces," *Phys. Rev. Applied*, vol. 2, p. 064002, Dec 2014.

[13] Y.-F. Zhu, X.-Y. Zou, R.-Q. Li, X. Jiang, J. Tu, B. Liang, and J.-C. Cheng, "Dispersionless manipulation of reflected acoustic wavefront by subwavelength corrugated surface," *Scientific reports*, vol. 5, p. 10966, 2015.

[14] G. Y. Song, B. Huang, H. Y. Dong, Q. Cheng, and T. J. Cui, "Broadband focusing acoustic lens based on fractal metamaterials," *Scientific reports*, vol. 6, no. 1, pp. 1–7, 2016.

[15] X. Wang, D. Mao, and Y. Li, "Broadband acoustic skin cloak based on spiral metasurfaces," *Scientific reports*, vol. 7, no. 1, p. 11604, 2017.

[16] Y. Ge, H.-x. Sun, S.-q. Yuan, and Y. Lai, "Broadband unidirectional and omnidirectional bidirectional acoustic insulation through an open window structure with a metasurface of ultrathin hooklike meta-atoms," *Applied Physics Letters*, vol. 112, no. 24, p. 243502, 2018.

[17] A. N. Norris, "Acoustic metafluids," *The Journal of the Acoustical Society of America*, vol. 125, pp. 839–849, feb 2009.

[18] U. Iemma and G. Palma, "Design of metacontinua in the aeroacoustic spacetime," *Scientific Reports*, vol. 10, p. 18192, 2020.

[19] R. Christie, A. Heidebrecht, and D. MacManus, "An Automated Approach to Nacelle Parameterization Using Intuitive Class Shape Transformation Curves," *Journal of Engineering for Gas Turbines and Power*, vol. 139, pp. 1–9, jun 2017.

[20] S. Rienstra and A. Hirschberg, *An Introduction to Acoustics*. Eindhoven University of Technology, 2004.

[21] W. Eversman, "Broadband noise suppression for turbofan inlet applications," *International Journal of Aeroacoustics*, vol. 15, no. 4-5, pp. 367–394, 2016.

[22] L. Heidelberg, "Fan Noise Source Diagnostic Test - Tone Modal Structure Results," in *8th AIAA/CEAS Aeroacoustics Conference & Exhibit*, (Reston, Virigina), pp. 1–21, American Institute of Aeronautics and Astronautics, jun 2002.

[23] A. Kempton, "Acoustic liners for modern aeroengines," in *15th CEAS-ASC workshop and 1st scientific workshop of x-noise EV, Switzerland*, 2011.

[24] J. Kennedy and R. Eberhart, "Particle swarm optimization," in *Proceedings of ICNN'95 - International Conference on Neural Networks*, vol. 4, pp. 1942–1948 vol.4, Nov 1995.